# Simplified sigmoidal curve fitting for a 6 MV FFF photon beam of Halcyon to determine the field size for beam commissioning and quality assurance

**Min-Geon Choi**
Catholic University of Korea School of Medicine
**Martin Law**
Proton Therapy Pte Ltd
**Do-Kun Yoon**
Catholic University of Korea School of Medicine
**Mikoto Tamura**
Kinki Daigaku - Osakasayama Campus
**Kenji Matsumoto**
Kinki Daigaku - Osakasayama Campus
**Masakazu Otsuka**
Kinki Daigaku - Osakasayama Campus
**Moo-Sub Kim**
Catholic University of Korea School of Medicine
**Shih-Kien Djeng**
Proton Therapy Pte Ltd
**Hajime Monzen**
Kinki Daigaku - Osakasayama Campus
**Tae Suk Suh** ( suhsanta@catholic.ac.kr )

**Research**

**Keywords:** Field Size, Sigmoidal Curve Fitting, FFF, Halcyon, Commissioning, QA

**Posted Date:** October 14th, 2020

**DOI:** https://doi.org/10.21203/rs.3.rs-21506/v3

**Version of Record:** A version of this preprint was published on December 7th, 2020. See the published version at https://doi.org/10.1186/s13014-020-01709-x.

# Abstract

Background : An O-ring gantry-type linear accelerator (Linac) with a 6 MV flattening filter-free (FFF) photon beam, Halcyon, includes a reference beam containing the representative information regarding the percent depth dose, profile, output factor, etc. for commissioning and quality assurance. However, because it does not provide the information of the field size, we proposed a method to determine all field sizes according to all depths for radiation therapy using simplified sigmoidal curve fitting (SCF). Methods : After a mathematical definition of the SCF using four coefficients, the defined curves were fitted to both the reference and measured data. For a high agreement between the fitting curve and the profiles in each data set, the field sizes were determined by identifying the maximum point along the third derivative of the fitting curve. The curve fitting included the field sizes for beam profiles of 2 × 2, 4 × 4, 6 × 6, 8 × 8, 10 × 10, 20 × 20 and 28 × 28 cm 2 as a function of depth (at 1.3, 5, 10, 20 cm). The results of the field size from the reference data were compared with the results in the measured data using the same condition. Results : All fitting curves show values of goodness of fit, R 2 , better than 0.99. The differences in the field size between the reference data and the measured data were within the range of 0 to 0.2 cm. The lowest difference in the field sizes at a depth of 10 cm, which is a surface-to-axis distance, was reported. Conclusion : The application of the SCF has been proven to accurately obtain the field size of the preconfigured reference and of the measured FFF photon beam data for the Halcyon system. The current work can be useful for beam commissioning as a counte-rcheck methodology to determine the field size from the reference data in the treatment planning system of a newly installed Halcyon system and for the routine quality assurance to ascertain the correctness of field sizes clinically used with the Halcyon system.


# Background

The field size of a radiation beam in radiotherapy with the use of a linear accelerator (linac) refers to the area for radiation delivery. For this reason, the determination of accurate field sizes is a significant parameter for the delivery of radiation and an important process in quality assurance (QA).[1, 2] Normally, the field size can be determined during a commissioning and QA procedure.[3, 4] While conventional linac systems have been equipped with a flattening filter (FF) type to deliver the radiation beam with a uniform dose distribution, the method of a full width at half maximum (FWHM) is the conventionally representative methodology for the determination of the field size for the FF beam.[5] The definition of the field size for the FF beam is based on a point off-axis at the dose of 50% after the dose normalization of a central axis (CAX) at 100%. This FWHM methodology is suitable for the determination of the field size of the FF beam since it has a uniform region around the CAX. According to the Task Group Report #142 of AAPM, several parameters, such as flatness, symmetry and penumbra, should be considered to characterize the FF beam.[6] In radiation therapy, the accuracy of the dose is a very important factor, and the treatment time also should not be overlooked. Since a long treatment time may cause patient discomfort and decrease the accuracy of treatment, the FFF beam is used to reduce treatment time. The FFF beam has the effect of reducing photon head scatter, leaf transmission head leakage, and the

peripheral dose.[7, 8] However, the method of FWHM is not suitable for determining the field size of the FFF beam, which shows a specific shape of the dose profile with relatively higher peak at the CAX.

The Halcyon system (Varian Medical Systems Inc., Palo Alto, USA), which is a linac with an O-ring gantry, is a radiotherapy machine using a 6 MV FFF beam, such as the Tomotherapy and Cyberknife systems. There have been several studies to define the field sizes of an FFF beam. The most representative method to determine the field size of the FFF beam is the use of the inflection point (IP) on the penumbra region of the beam's profile.[9, 10] Nevertheless, there are some uncertainties in obtaining a correct IP from beam data measurement. To consider this uncertainty, Pönisch et al. proposed a method to identify the IP at the field edge of the FFF beam with the same level of the FF beam. The position of the IP can be different according to the positional step size error to obtain the beam profile.[11] Fogliata et al. suggested the formulation of renormalization to overcome the uncertainty in IP due to the stepping size.[12] Basically, although these two methods to define the field size of the FFF beam are originally based on the profiles of the FF beam, with the large number of values, both methods still exhibit a position error in the measurement. The parameterized gradient-based method (PGM) that complements these two methods was proposed to determine the field size of the FFF beam using a mathematical model.[13, 14] However, the parameters of the profile were partially reported. In addition, since the PGM method also applied a mathematical model that originated from the measured data, the uncertainty of the measurement still exists, as in the initial two methods. When the users of the Halcyon system use our proposed method to determine the field size, there are several convenient points. First, we proposed a reasonable method to determine the field size of the halcyon beam according to all depths and all field sizes. The vendor of the Halcyon already entered all beam data to the TPS. In addition, they provide reference data (RD), such as the PDD, profiles and output factors. This RD is used to optimize and calculate the dose, which is effective for the operation of the Halcyon system in the Eclipse TPS. However, because this vendor does not provide any information of the field size in the RD, the field size should be determined by their method for all conditions. In this study, one of the methods for determining the effective value for the field size with a simple mathematical equation was employed for all of depths as well as all field sizes.

Second, we used the RD from the vendor to determine the field size and dose without using our measured data. The commissioning procedure in the Halcyon system provides the opportunity to verify the reliability and accuracy of the beam data by comparing with the agreement between the RD and measured data by the Halcyon's users. The vendor of the Halcyon system is continuously increasing the reliability of quality control by providing updated information regarding the RD to the Halcyon's users. Our research is to carry out fitting on the premise that the data provided by the vendor is correct, since the conventional linac has the possibility of errors caused by several conditions. When we measure the data for the additional commissioning procedure or the QA steps, we can check the accuracy of the field size using the reference value from the RD.

Last, we used methodology using only the sigmoid function without any other equations to generate the fitting curve on the beam profile. The procedure for the proposed method applicable to the RD has been simplified compared with the procedure of the PGM.[15-17]

# Methods

## 2.1 Preparation of data

A preconfigured reference beam dataset (reference data) generated by the vendor is stored in the treatment planning system when a new Halcyon system is installed. The reference data includes the lateral dose profiles for field sizes of 2 × 2, 4 × 4, 6 × 6, 8 × 8, 10 × 10, 20 × 20 and 28 × 28 $cm^2$ as a function of depth at 1.3, 5, 10, and 20 cm into the water phantom. To compare the field size from the reference data with that from the measured data, the measurement was performed under the same conditions as the reference data. The source-to-surface distance (SSD) was set at 90 cm. The CC13 ionization chamber and the Blue Phantom water tank (IBA Dosimetry, Schwarzenbruck, Germany) were used to measure the relative dose profiles for field sizes > 4 × 4 $cm^2$. For field sizes ≤ 4 × 4 $cm^2$, an edge diode detector (Sun Nuclear, Melbourne, FL, USA) was used. The scanning step for the acquisition of the profile on the measurement line along the off-axis position was 0.1 cm. All measurement values were processed by using OminiPro Accept7 (version 7.4.24.0) software (IBA dosimetry, Schwarzenbruck, Germany).

## 2.2 Definition of fitting using sigmoidal curve

The sigmoidal curve originates from the sigmoid function, which has been used at the field of the signal process. The shape of the sigmoidal curve is given by Eq.(1), (see Equation 1 in the Supplementary Files)

The coefficients α, β, γ, and δ are used to determine the shape of the curve *f(x)*. The coefficient α controls the gradient of the sigmoidal curve. The higher value of α makes the curve gradient steeper. The coefficient β is related to the horizontal movement of the whole sigmoidal curve. The higher value of β lets the sigmoidal curve move further to the right hand side of the curve. The coefficient γ determines the location of the only upper end of the sigmoidal curve. The higher value of γ lets the upper end of the sigmoidal curve occur at a higher position. The coefficient δ determines the vertical movement of the whole sigmoidal curve. The higher value of δ lets the sigmoidal curve move to a more upward direction. Thus, the coefficients α and γ contribute to transforming the shape of the curve. The coefficients β and δ change the location of the sigmoidal curve.

After the upload of the profile to MATLAB (2019 version, MathWorks Inc, Sherborn, MA, USA), the SCF was performed by the change in each coefficient until the sigmoidal curve overlapped on the profile. Basically, both terminal points of the virtual fitting curve should be located on the RD curve. In that case, the slope of the virtual fitting curve also should be matched with the slope of the RD curve. For all processes, we could change the coefficients for the sigmoid equation to edit the shape of the fitting curve. If the fitting curve is normal, we can see the S-shaped curve, which is exactly overlapped on the RD curve.

## 2.3 Verification of agreement for fitting curves

To verify the accuracy of the fitting curve based on the sigmoidal curve with the profiles, the average agreement ratio (AAR) between the values in the fitting curve ($f_i$) and the values in the profiles ($x_i$) at the same step position were calculated using Eq. (2), which shows the agreement between values from the profile and fitting. (see Equation 2 in the Supplementary Files)

In this study, if the AAR is higher than 97%, the optimization for the fitting terminates because the sufficient accuracy for the fitting has been obtained and the four coefficients (α, β, γ, and δ) are used to define shape of the final fitting curve. Moreover, an additional verification was performed through the evaluation of goodness of fit, $R^2$ (Eq. (3)) (see Equation 3 in the Supplementary Files)

where  is the mean of all $f_i$ values on the fitting curve, and $y_i$ is a value on the profile. The same validation procedures were applied to the measured data and to the reference data.

### 2.4 Identification of specific regions & points

In this study, in order to describe the sigmoidal curve, three regions and two points were assigned for the definition of the half-side of the SCF (fig. 1(a)). The three regions include the introductory region (IR), the growing region (GR), and plateau region (PR). The IR is the region starting to increase on the sigmoidal curve. The GR is a continuously increasing region on the sigmoidal curve. The PR is the region slowing down to increase. These regions can be identified through the second derivative of the sigmoidal curve, as shown Fig. 1(a). The range between the rightmost point and the maximum point on the second derivative curve was defined as the IR. The range between the maximum point and the minimum point on the second derivative curve was defined as the GR. The region between the minimum point and the leftmost point on the second derivative curve was defined as the PR. Because of the specification of the sigmoidal shape, there are two specific points as the singular point (SP) and inflection point (IP), both of which could be identified from the third derivative curve of the sigmoidal curve. The SP is the minimum point between the range of the IR and the GR (Eq. (4)). The IP is another minimum point in the range between the GR and the PR, as shown in Eq. (5). When there is no point in either the IP or the SP, the re-fitting process was performed from section 2.2. (see Equations 4 and 5 in the Supplementary Files)

### 2.5 Determination of the Field Size

Although the determined field size (DFS) can be calculated using only the first derivative, the second and third derivatives give the opportunity to check whether this DFS exists in the period between IP and SP and to check the error of the fitting curve. Due to incorrect fitting or an insufficient fitting range for the first derivative, it can be defined as the wrong field size. In the extreme case, the IP and the SP cannot be found on the derivative curve. As a result, the DFS cannot be calculated. If we determine the field size using only the first derivative, the results have some uncertainties. Therefore, the purpose of the second derivative is to check the presence of both the IP and the SP. Last, the purpose of the third derivative is to determine the DFS for the clear periods between the IP and the SP. Because the right third derivative curve can show these three points at one clip, the determination of the field size using the third derivative curve is most efficient. After the SP and the IP have been obtained, the DFS can be identified as the maximum

point on the third derivative curve between the SP and the IP, as shown below in Eq. (6). Figure 1(b) shows the conceptual DFS on the third derivative curve, and an actual example of the DFS has been demonstrated by fitting to the profile in Fig. 1(b) (see Equation 6 in the Supplementary Files)

The factor 2 in the equation (Eq. (6)) is present because only the right hand half side of the symmetric open beam profile was used for the curve fitting.

# Results

### 3.1 The Accuracy of the fitting curve

Figure 2 shows all the final fitting curves using SCF with half of the profiles in the reference data. The profiles for all field sizes (2 × 2, 4 × 4, 6 × 6, 8 × 8, 10 × 10, 20 × 20, and 28 × 28 $cm^2$) are demonstrated as a function of depth (1.3, 5, 10, and 20 cm) as (a), (b), (c), and (d), respectively. The fitting curve is indicated by the red circles on each profile. On the other hand, Figure 3 shows all the final fitting curves using same SCF with the half of profiles in the measured data. It also includes the profiles for all field sizes with variable depths: 1.3, 5, 10, and 20 cm as (a), (b), (c), and (d), respectively. The profiles in Fig. 2 and 3 along the field size are distinguished by their color and have been normalized by relative dose at the CAX. The X-axis shows the off-axis position from the CAX. All the fitting curves show good agreement with each profile. The accuracy for all fitting curves were evaluated using the method of AAR and $R^2$. The performances were reported as over 0.99 for $R^2$.

Table 1 tabulates all coefficients to form the final sigmoidal curves for all field sizes with all depths using SCF before determination of the field size. The differences of the coefficient values at all depths were reported as α maximum difference 1.3, β maximum difference 4.4, γ maximum difference 4.0, δ maximum difference 1.7, and all coefficients had a minimum difference of 0. All values for IP and SP were also tabulated. The maximum and minimum differences for the results in IP were 0.15 cm and 0 cm, respectively. The maximum and minimum differences for the results in SP were 0.18 cm and 0 cm, respectively.

**Table 1. Comparison between reference data and measured data for all coefficients and IP, SP**

| | Field Size | RD | MD | RD | MD | RD | MD | RD | MD | RD | MD | RD | MD |
|---|---|---|---|---|---|---|---|---|---|---|---|---|---|
| | ($cm^2$) | α | α | β | β | γ | γ | δ | δ | IP (cm) | IP (cm) | SP (cm) | SP (cm) |
| Depth 1.30 cm | 2 × 2 | 11.20 | 9.90 | -10.30 | -9.20 | 97.50 | 97.50 | 1.80 | 2.00 | 0.69 | 0.66 | 1.10 | 1.14 |
| | 4 × 4 | 10.00 | 8.80 | -18.30 | -16.20 | 97.50 | 93.50 | 2.30 | 4.00 | 1.58 | 1.56 | 2.03 | 2.08 |
| | 6 × 6 | 6.06 | 5.20 | -16.50 | -14.50 | 94.50 | 93.00 | 2.90 | 4.00 | 2.32 | 2.32 | 3.08 | 3.20 |
| | 8 × 8 | 6.03 | 5.70 | -22.00 | -20.60 | 92.00 | 93.00 | 3.30 | 2.80 | 3.24 | 3.19 | 4.00 | 3.99 |
| | 10 × 10 | 6.01 | 6.30 | -27.50 | -27.80 | 89.50 | 89.60 | 3.20 | 3.00 | 4.17 | 4.02 | 4.93 | 4.75 |
| | 20 × 20 | 5.85 | 5.90 | -53.50 | -53.80 | 73.00 | 73.00 | 4.90 | 5.00 | 8.91 | 9.01 | 9.78 | 9.80 |
| | 28 × 28 | 5.70 | 5.90 | -72.30 | -74.90 | 62.50 | 62.50 | 5.00 | 5.00 | 12.37 | 12.28 | 13.18 | 13.06 |
| Depth 5.00 cm | 2 × 2 | 10.20 | 9.80 | -9.80 | -9.20 | 95.00 | 95.00 | 3.50 | 3.40 | 0.71 | 0.68 | 1.16 | 1.15 |
| | 4 × 4 | 10.00 | 9.40 | -19.00 | -17.40 | 90.50 | 90.70 | 5.90 | 4.70 | 1.65 | 1.58 | 2.10 | 2.07 |
| | 6 × 6 | 5.50 | 5.30 | -15.60 | -14.80 | 91.00 | 91.00 | 5.00 | 4.60 | 2.39 | 2.33 | 3.23 | 3.20 |
| | 8 × 8 | 5.30 | 5.30 | -20.10 | -19.90 | 88.00 | 88.00 | 6.00 | 5.40 | 3.33 | 3.30 | 4.20 | 4.16 |
| | 10 × 10 | 5.30 | 4.80 | -25.20 | -24.60 | 84.30 | 85.80 | 6.30 | 5.90 | 4.30 | 4.21 | 5.12 | 5.16 |
| | 20 × 20 | 5.10 | 5.10 | -48.30 | -48.40 | 70.00 | 69.60 | 7.20 | 7.20 | 9.00 | 9.02 | 9.93 | 9.91 |
| | 28 × 28 | 5.00 | 5.00 | -66.50 | -66.30 | 60.00 | 59.50 | 7.00 | 6.80 | 12.82 | 12.78 | 13.73 | 13.69 |
| Depth 10.00 cm | 2 × 2 | 8.70 | 8.80 | -8.70 | -8.80 | 96.00 | 96.40 | 3.50 | 2.10 | 0.73 | 0.71 | 1.22 | 1.24 |
| | 4 × 4 | 9.00 | 8.80 | -18.10 | -17.50 | 90.00 | 88.50 | 6.00 | 6.90 | 1.73 | 1.70 | 2.24 | 2.22 |
| | 6 × 6 | 5.50 | 5.10 | -16.40 | -15.10 | 88.00 | 88.00 | 7.30 | 6.80 | 2.54 | 2.49 | 3.37 | 3.39 |
| | 8 × 8 | 5.10 | 4.90 | -20.40 | -19.40 | 86.50 | 84.80 | 7.40 | 7.60 | 3.53 | 3.47 | 4.42 | 4.40 |
| | 10 × 10 | 5.10 | 4.60 | -25.50 | -22.80 | 81.80 | 91.00 | 8.30 | 9.00 | 4.53 | 4.51 | 5.42 | 5.44 |
| | 20 × 20 | 4.90 | 4.90 | -48.80 | -48.90 | 64.70 | 63.60 | 10.60 | 10.60 | 9.47 | 9.49 | 10.40 | 10.42 |
| | 28 × 28 | 4.80 | 4.80 | -67.30 | -66.90 | 53.50 | 53.50 | 10.50 | 10.50 | 13.52 | 13.43 | 14.47 | 14.39 |
| Depth 20.00 cm | 2 × 2 | 7.80 | 7.70 | -8.65 | -8.50 | 94.50 | 96.20 | 4.00 | 2.90 | 0.79 | 0.78 | 1.38 | 1.38 |
| | 4 × 4 | 7.50 | 7.10 | -16.50 | -15.50 | 89.70 | 89.40 | 7.30 | 7.30 | 1.87 | 1.84 | 2.48 | 2.48 |
| | 6 × 6 | 4.80 | 4.80 | -15.80 | -15.30 | 97.00 | 86.30 | 8.40 | 8.70 | 2.79 | 2.72 | 3.74 | 3.71 |
| | 8 × 8 | 4.80 | 4.80 | -21.10 | -21.20 | 82.00 | 79.20 | 10.50 | 11.40 | 3.89 | 3.91 | 4.85 | 4.87 |
| | 10 × 10 | 4.90 | 4.10 | -26.90 | -22.50 | 75.50 | 76.00 | 13.50 | 13.00 | 5.00 | 4.90 | 5.93 | 6.02 |
| | 20 × 20 | 4.75 | 5.00 | -54.30 | -55.00 | 56.00 | 54.30 | 16.00 | 16.40 | 9.62 | 9.60 | 10.45 | 10.40 |
| | 28 × 28 | 5.00 | 5.00 | -77.00 | -77.00 | 45.50 | 45.00 | 15.50 | 15.50 | 14.22 | 14.22 | 14.68 | 14.70 |

Table 2 tabulates all values for DFS from the fitting curve to all profiles at different depths. For the field sizes, the maximum difference was 0.2 cm and the minimum difference was 0 cm. The results for a depth of 10 cm showed the least difference between the reference data and the measured data.

**Table 2**. Determination of field size for reference data and measured data

| | Field Size ($cm^2$) | RD DFS (cm) | MD DFS (cm) |
|---|---|---|---|
| Depth 1.30 cm | 2 × 2 | 1.80 | 1.82 |
| | 4 × 4 | 3.64 | 3.66 |
| | 6 × 6 | 5.42 | 5.54 |
| | 8 × 8 | 7.26 | 7.20 |
| | 10 × 10 | 9.12 | 9.00 |
| | 20 × 20 | 18.18 | 18.20 |
| | 28 × 28 | 25.56 | 25.36 |
| Depth 5.00 cm | 2 × 2 | 1.90 | 1.84 |
| | 4 × 4 | 3.76 | 3.68 |
| | 6 × 6 | 5.64 | 5.56 |
| | 8 × 8 | 7.56 | 7.48 |
| | 10 × 10 | 9.44 | 9.38 |
| | 20 × 20 | 18.94 | 18.96 |
| | 28 × 28 | 26.56 | 26.50 |
| Depth 10.00 cm | 2 × 2 | 1.98 | 1.96 |
| | 4 × 4 | 4.00 | 3.94 |
| | 6 × 6 | 5.94 | 5.90 |
| | 8 × 8 | 7.96 | 7.88 |
| | 10 × 10 | 9.96 | 9.98 |
| | 20 × 20 | 19.88 | 19.92 |
| | 28 × 28 | 28.02 | 27.96 |
| Depth 20.00 cm | 2 × 2 | 2.18 | 2.18 |
| | 4 × 4 | 4.38 | 4.34 |
| | 6 × 6 | 6.56 | 6.44 |
| | 8 × 8 | 8.76 | 8.80 |
| | 10 × 10 | 10.94 | 10.94 |
| | 20 × 20 | 21.68 | 21.90 |
| | 28 × 28 | 30.76 | 30.96 |

# Discussion

There have been previous studies on the determination of the field size of the conventional FF beam, such as the FWHM, which is not suitable for the Halcyon linac's profile due to the difference in the CAX of the dose. The limitation of the current measurement is that it is time consuming to apply a fine scanning step of 0.1 cm in the QA and commissioning process. MSM, techniques by Pönisch et al. and the method of the renormalization, which are typical definition methods for the FFF beam field size, could contain uncertainty arising from the scanning step.[9-12] The uncertainty at the location of the inflection point may occur from the measured data due to using a less fine scanning step. On the other hand, although the PGM method shows the advantage in that it does not affect to the size of scanning step, its analytical fitting also obtained the parameters from the measured data.[13, 14] Thus, all studies on the field size definition described above defined the field size based on the data measured by the user, whereas our study defined the field size using the RD representing the characteristics of the Halcyon system. This means that the consistency of the beam data is guaranteed in all institutions using the Halcyon system, and the Halcyon field size data we propose using mathematical fitting curves ensures high accuracy and reliability; commissioning and QA of each institution could be reference data.[15-18]

In the case of PGM, the field size of the measured data was largely separated as 4 × 4 $cm^2$< and 4 × 4 $cm^2$> to obtain the coefficient from the measured data. However, the coefficient for 2 × 2 $cm^2$ and 2.5 ×

2.5 $cm^2$ in the calculated data, which is used to check the coefficient accuracy of the measured data are not presented. Although it does not rule out the possibility of equipment-specific changes, the field size of the small field is an important factor for any vendor's equipment.[13, 14, 19] Thus, we proposed determining all coefficients and all field sizes, including the small field, for the FFF beam-only Halcyon system.

The physicists must counter-check the installed beam data. The method described in the manuscript not only provides an independent QA/QC method for the installed beam data and a method as a QA tool to provide QA/QC for the installed beam data as an independent methodology towards the routine service of the Halcyon system.

It is meaningful in that the criteria can be established through the use of the reference data. This work with adequate parameters information and simple methodology could be useful, especially for new Halcyon users who must perform the validation of the preconfigured reference for the beam commissioning process as well as the QA because beam data can vary from machine to machine of the same model and same vendor, as described by AAPM TG,51,100,106.[17, 18, 20]

# Conclusions

The determination of the field size using the simple SCF method has been established for a radiation beam of 6 MV FFF from the Halcyon system. This method covers all field sizes, including small field sizes. The coefficients for the fitting and field sizes between the reference data and the measured data were in good accord and can be used as a repeated countercheck for other users using the same model of linac.

# List Of Abbreviations

QA: Quality assurance; IMRT: Intensity modulated radiation therapy; VMAT: Volumetric modulated arc therapy, SCF: Sigmoidal fitting curve; RD: Reference data; MD: Measured data; AAR: Average agreement ratio; IR: Introductory region; GR: Growing region; PR: Plateau region; SP: Singular point; IP: Inflection point; DFS: Determined field size

# Declarations

### Ethics approval and consent to participate

Not applicable

### Consent for publication

Not applicable

### Availability of data and materials

The datasets used and/or analyzed during the current study are available from the corresponding author on reasonable request.

### Competing interests

The authors declare that they have no competing interests.


### Funding

This research was supported by National Research Foundation of Korea Grant

Funded by the Korean Government (2018A2B2005343).


### Authors' contribution

Study concept and design: MC, DY, MT, HM, TS. Data acquisition: MT, KM, MO, HM. Data analysis and interpretation: MC, DY, ML, MT, KM, MO, MK, SKD, HM, TS. Computer program modeling: MC, DY, MK. Manuscript preparation and editing: MC, ML, DY, MT, HM, TS. Manuscripts review: All authors read and approved the final manuscript.


### Acknowledgements

Not applicable.


## References


[1] Kry SF, Dromgoole L, Alvarez P, Leif J, Molineu A, Taylor P, et al. Radiation therapy deficiencies identified during on-site dosimetry visits by the imaging and radiation oncology core Houston quality assurance center. Int J Radiat Oncol Biol Phys. 2017;99:1094-100.

[2] Sun B, Goddu SM, Yaddanapudi S, Noel C, Li H, Cai B, et al. Daily QA of linear accelerators using only EPID and OBI. Med Phys. 2015;42:5584-94.

[3] Hrbacek J, Lang S, Klöck S. Commissioning of photon beams of a flattening filter-free linear accelerator and the accuracy of beam modeling using an anisotropic analytical algorithm. Int J Radiat Oncol Biol Phys. 2011;80:1228-37.

[4] Shende R, Gupta G, Patel G, Kumar S. Commissioning of TrueBeam TM Medical Linear Accelerator: Quantitative and Qualitative Dosimetric Analysis and Comparison of Flattening Filter (FF) and Flattening Filter Free (FFF) Beam. IJMPCERO. 2016;5:51.

[5] Chang K-P, Wang Z-W, Shiau A-C. Determining optimization of the initial parameters in Monte Carlo simulation for linear accelerator radiotherapy. RADIAT

PHYS CHEM. 2014;95:161-5.

[6] Klein EE, Hanley J, Bayouth J, Yin FF, Simon W, Dresser S, et al. Task Group 142 report: Quality assurance of medical acceleratorsa. Med Phys. 2009;36:4197-212.

[7] Stieler F, Fleckenstein J, Simeonova A, Wenz F, Lohr F. Intensity modulated radiosurgery of brain metastases with flattening filter-free beams. Radiother Oncol.. 2013;109:448-51.

[8] Cho W, Kielar KN, Mok E, Xing L, Park JH, Jung WG, et al. Multisource modeling of flattening filter free (FFF) beam and the optimization of model parameters. Med Phys. 2011;38:1931-42.

[9] Muralidhar K. Derivation of equations to define inflection point and its analysis in flattening filter free photon beams based on the principle of polynomial function. Int J Cancer Ther Oncol. 2015;3:03015.

[10] Pichandi A, Ganesh KM, Jerin A, Balaji K, Kilara G. Analysis of physical parameters and determination of inflection point for Flattening Filter Free beams in medical linear accelerator. Rep Pract Oncol Radiother. 2014;19:322-31.

[11] Pönisch F, Titt U, Vassiliev ON, Kry SF, Mohan R. Properties of unflattened photon beams shaped by a multileaf collimator. Med Phys. 2006;33:1738-46.

[12] Fogliata A, Garcia R, Knöös T, Nicolini G, Clivio A, Vanetti E, et al. Definition of parameters for quality assurance of flattening filter free (FFF) photon beams in radiation therapy. Med Phys. 2012;39:6455-64.

[13] Lebron S, Lu B, Yan G, Kahler D, Li JG, Barraclough B, et al. Parameterization of photon beam dosimetry for a linear accelerator. Med Phys. 2016;43:748-60.

[14] Lebron S, Yan G, Li J, Lu B, Liu C. A universal parameterized gradient-based method for photon beam field size determination. Med Phys. 2017;44:5627-37.

[15] De Roover R, Crijns W, Poels K, Michiels S, Nulens A, Vanstraelen B, et al. Validation and IMRT/VMAT delivery quality of a preconfigured fast-rotating O-ring linac system. Med Phys. 2019;46:328-39.

[16] Netherton T, Li Y, Gao S, Klopp A, Balter P, Court LE, et al. Experience in commissioning the halcyon linac. Med Phys. 2019;46:4304-13.

[17] Teo PT, Hwang MS, Shields W, Kosterin P, Jang SY, Heron DE, et al. Application of TG-100 risk analysis methods to the acceptance testing and commissioning process of a Halcyon linear accelerator. Med Phys. 2019;46:1341-54.

[18] Lloyd SA, Lim TY, Fave X, Flores-Martinez E, Atwood TF, Moiseenko V. TG-51 reference dosimetry for the Halcyon™: a clinical experience. J Appl Clin Med Phys. 2018;19:98-102.

[19] Das IJ, Ding GX, Ahnesjö A. Small fields: nonequilibrium radiation dosimetry. Med Phys. 2008;35:206-15.

[20] Das IJ, Cheng CW, Watts RJ, Ahnesjö A, Gibbons J, Li XA, et al. Accelerator beam data commissioning equipment and procedures: report of the TG-106 of the Therapy Physics Committee of the AAPM. Med Phys. 2008;35:4186-215.

# Figures

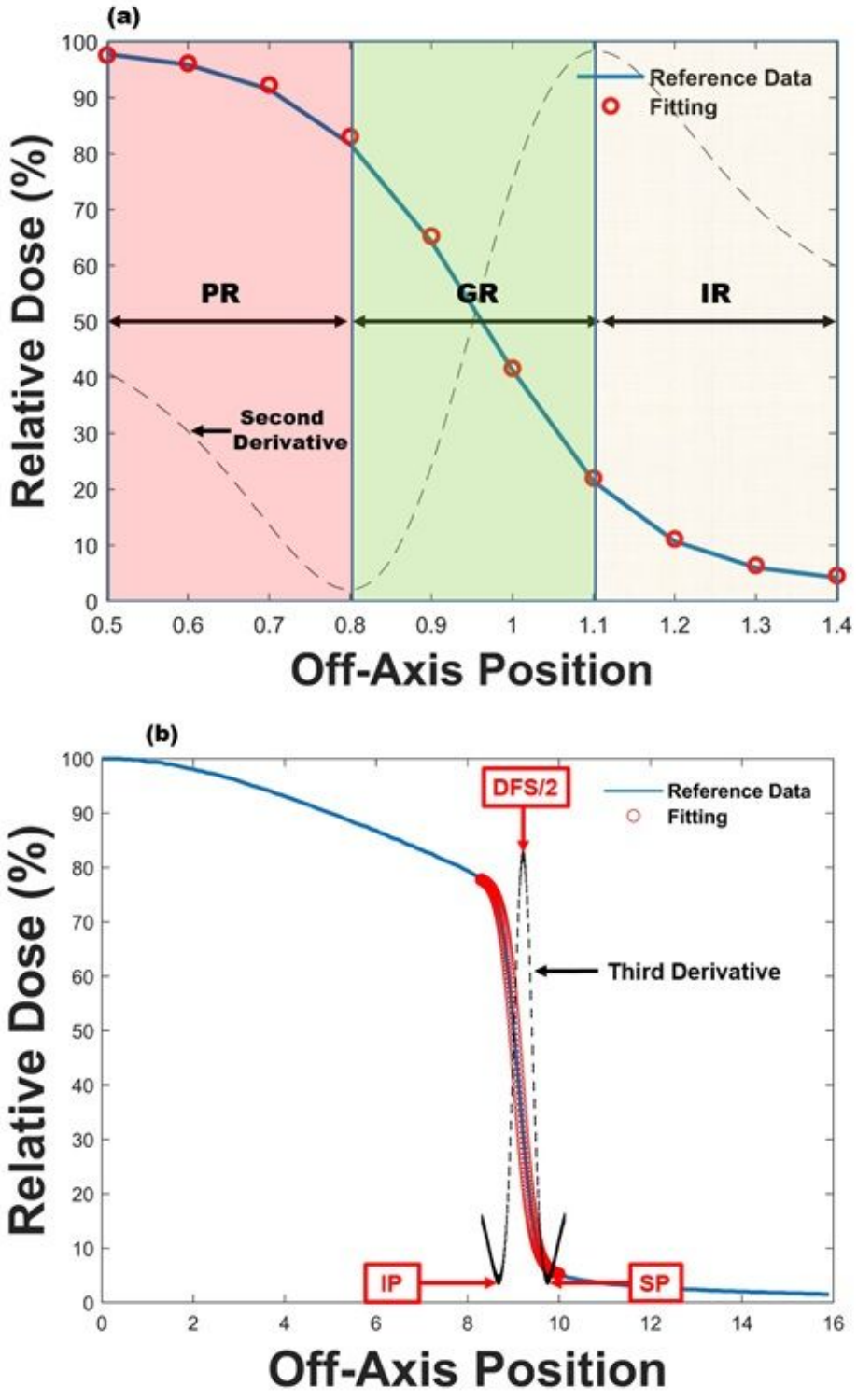


**Figure 1**

(a) An example for explaining the method for the identification of three region and two specific points. The three regions were defined by the second derivative and the two specific points were set at the minimum points of the third derivative curve: Identification of the position for the introductory region (IR; Yellow region), the growing region (GR; Green region), and plateau region (PR; Red region). (b) The singular point (SP) and the inflection point (IP). The red dots show the fitting curve on the profile (Blue line). The black dotted line shows the shape of the third derivative curve. A comparison of the whole fitting curve with the third derivative: the positions for the SP, IP, and DFS/2 on the black dotted line are shown.

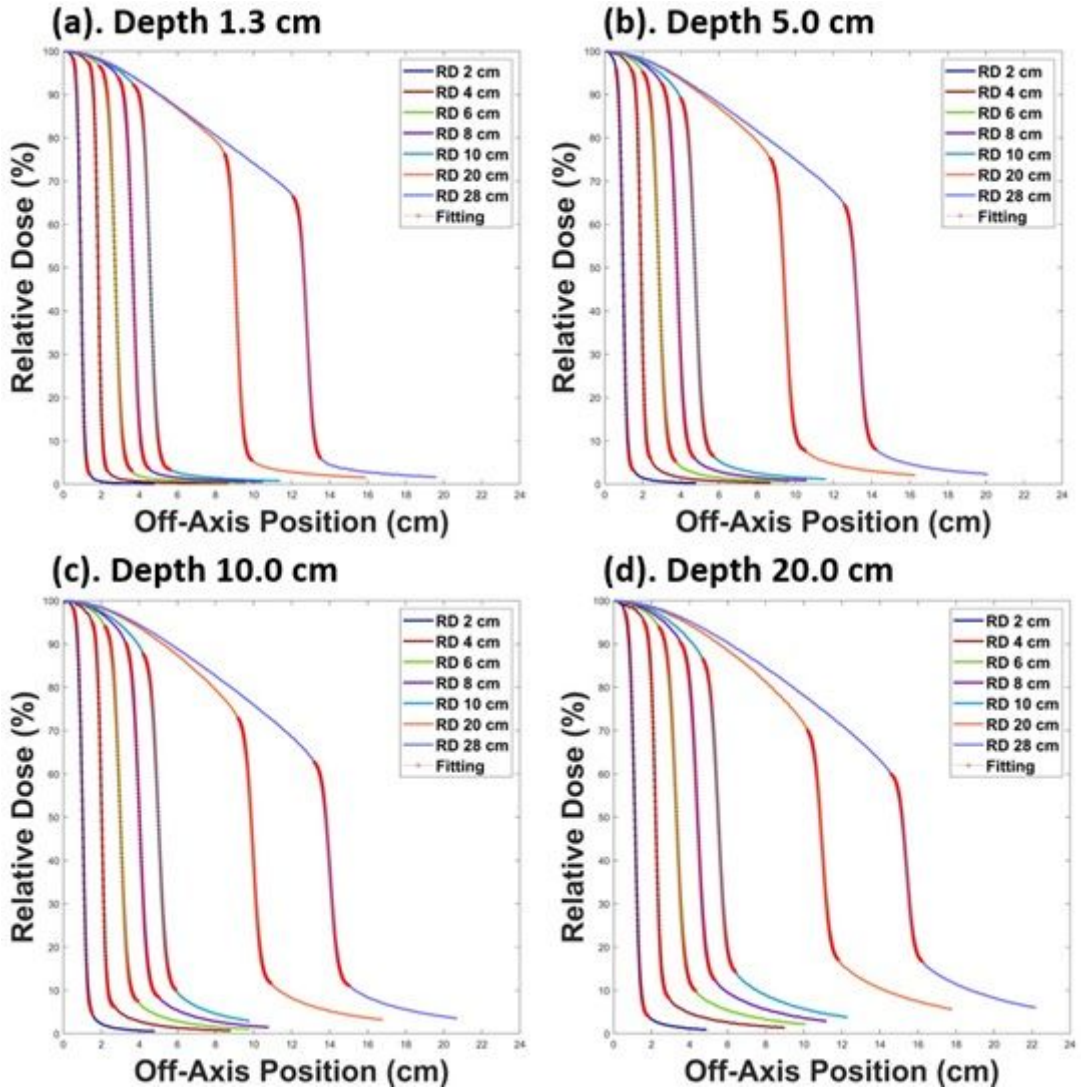


## Figure 2

The fitting curves and the profiles from the reference data (RD). The profiles according to the field sizes of 2 × 2, 4 × 4, 6 × 6, 8 × 8, 10 × 10, 20 × 20, and 28 × 28 cm2 along with the fitting curves for each beam profile (red circles). The depths for the profiles are (a) 1.3 cm, (b) 5 cm, (c) 10 cm, and (d) 20 cm.

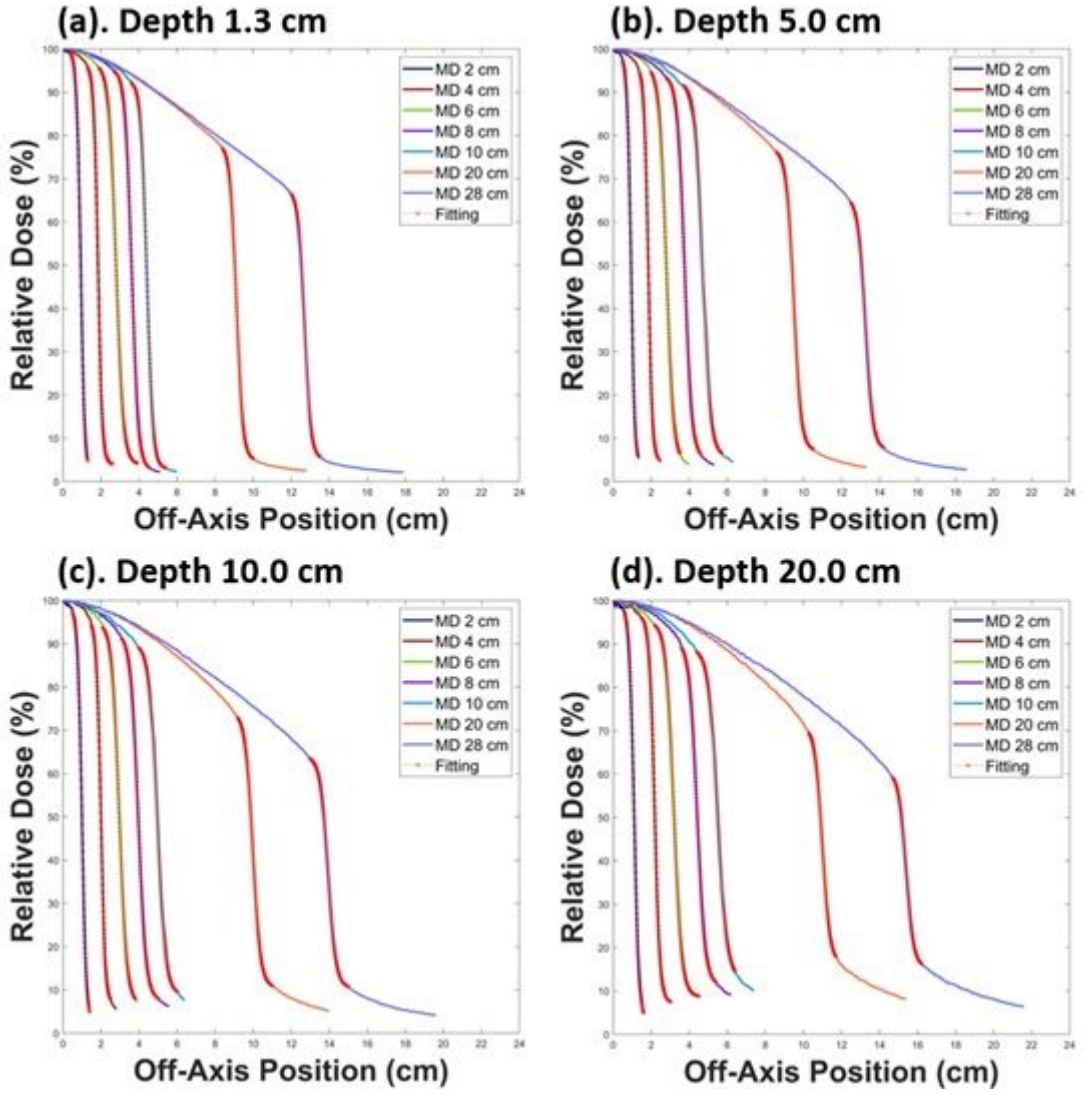


**Figure 3**

The fitting curves and the profiles from the measured data (MD). The profiles according to the field sizes of 2 × 2, 4 × 4, 6 × 6, 8 × 8, 10 × 10, 20 × 20, and 28 × 28 cm2 along with the fitting curves for each beam profile (red circles). The depths for the profiles are (a) 1.3 cm, (b) 5 cm, (c) 10 cm, and (d) 20 cm.

# Supplementary Files

This is a list of supplementary files associated with this preprint. Click to download.

- Equations.pdf